Inertial range determination for aerothermal turbulence using fractionally differenced processes and wavelets

W. Constantine* and D. B. Percival†
Insightful Corporation, Suite 500, 1700 Westlake Avenue North, Seattle, Washington 98109-3044

P. G. Reinhall
Department of Mechanical Engineering 356200, University of Washington, Seattle, Washington 98195
(Received 6 February 2001; published 14 August 2001)

A fractionally differenced (FD) process is used to model aerothermal turbulence data, and the model parameters are estimated via wavelet techniques. Theory and results are presented for three estimators of the FD parameter: an ''instantaneous'' block-independent least squares estimator and block-dependent weighted least squares and maximum likelihood estimators. Confidence intervals are developed for the block-dependent estimators. We show that for a majority of the aerothermal turbulence data studied herein, there is a strong departure from the theoretical Kolmogorov turbulence over finite ranges of scale. A time-scale-dependent inertial range statistic is developed to quantify this departure.

DOI: 10.1103/PhysRevE.64.036301 PACS number(s): 47.53.+n, 47.27.−i, 89.75.Kd

I. INTRODUCTION

The last three decades have seen a rapid advance in the mathematical modeling of turbulence data. Encouraged partly by the fact that complex, seemingly random, behavior can be well modeled by simple low-dimensional deterministic nonlinear systems, many researchers have hypothesized that turbulence can be modeled using chaos theory. Early experiments in Rayleigh-Bernard thermal convection [1], Taylor-Couette flow between cylinders [2], closed loop thermosiphons [3], turbulent boundary layers for open flow over a wall [4], and surface wave propagation in a saltwater medium [5], have in the part verified this hypothesis. However, there is a lack of such clear proof in other experiments and in data collected from uncontrolled environments such as in aerothermal data. More recent efforts in turbulence modeling have shown chaos theory to be useful in interpreting local phenomenon and flow stability. Chaos is now generally considered to have an important (yet limited) role in the modeling of turbulence but not as a theory capable of describing turbulent flow in detail. Even if the turbulence is viewed as a deterministic event, the high degrees of freedom (dimension) of the flow makes the use of chaos theory impractical. Hence, the treatment of turbulence as a stochastic process prevails and (similarly to low-dimensional chaotic models) is well matched for handling a prevalent notion about turbulence, namely, that it has certain ''self-similar'' or ''fractal'' properties. Loosely speaking, this property means that certain measures of turbulence data are invariant upon rescaling the data, but the measures are quite different for stochastic and deterministic models (e.g., invariance in distributional properties in the former and invariance in space-filling properties in the latter). Both approaches are capable of generating simulated series that mimic some properties of actual turbulence, but there is much work yet to be done to ascertain which class of models or combination thereof is the best to use to answer questions of practical importance.

Most deterministic and stochastic approaches assume homogeneity in time across all scales of interest. In this paper, we discuss methods that can be used for turbulence with time-varying properties. As we show below, there is strong evidence to support the notion that turbulence measurements such as we consider here exhibit time varying power law behavior over finite ranges of scale. Because of the temporally localized and scale-dependent nature of wavelet transforms, wavelet techniques provide a natural framework for the analysis of physical phenomena that exhibit variations across time and within a finite range of scales. This is a departure from techniques that assume *a priori* either a self-similar structure across all scales in the data or stationarity in fractal measures as a function of time (see Refs. [6–9] for examples of wavelet-based estimation of nontime varying turbulence model parameters). While a wavelet decomposition of a turbulence time series, say $\{X_t\}$, is based on using self-similar analysis tools (i.e., wavelets), it does *not* make an *a priori* assumption that $\{X_t\}$ is evolving in a self-similar manner. By making a careful study of each scale as it evolves in time and of the relationships of the scales to each other, we can then evaluate how reasonable it is to use models that postulate a tight coupling across scales, e.g., time-evolving power law processes.

In this article, we use recently developed wavelet techniques to estimate the parameters of fractionally differenced (FD) processes applied to aerothermal turbulence data. There are a number of advantages in using the discrete wavelet transform (DWT) on turbulence data.

Decomposition based on scale. Turbulence is known to exhibit fluctuations at various spatial scales, and hence the DWT is a natural analyzer.

Decorrelation of time series. While turbulence data are typically highly correlated, their wavelet coefficients are approximately uncorrelated [10] (see Sec. IV C for details). This property is crucial for obtaining viable approximate

*Electronic address: wconstan@insightful.com
†Also at Applied Physics Laboratory, Box 355640, University of Washington, Seattle, WA 98195-5640.

maximum likelihood estimates of FD parameters.

Localized time and scale content. Each wavelet coefficient is localized in time, allowing us to track changes in the characteristics of a time series at a particular scale as a function of time.

Separation of nonlinear trends from noise. The wavelet coefficients are inherently ''blind'' (invariant) to nonlinear polynomial trend contamination in the original time series [11].

As in Refs. [12,13], we use wavelet techniques to analyze intermittent deviations from Kolmogorov inertial subrange behavior for measured temperature-based turbulence data. We extend these works by (1) using higher order wavelet filters (non-Haar wavelets) to avoid spurious estimates of model parameters, (2) refining novel block estimation techniques with weighted least squares and maximum likelihood estimators, (3) developing an instantaneous (block-independent) least squares estimator, (4) using simple diagnostic statistics as a means of identifying anomalous deterministic structure imposed by the measurement system (thereby helping us to eliminate scales over which a stochastic fractal model is inappropriate), and (5) developing confidence intervals for the block-dependent estimators.

The remainder of this paper is organized as follows. In Sec. II we define an FD process and discuss why it has certain advantages over other models that have been used with turbulence data. In Sec. III we define the specific wavelet transforms used herein, including the DWT and a related nondecimated transform (the ''maximal overlap'' DWT) that allows us to define an ''instantaneous'' estimator of FD parameters as a function of time. In Sec. IV we discuss wavelet transform techniques for estimating the FD parameters for turbulence data—these include a block-dependent weighted least squares estimator (Sec. IV A), a block-independent least squares estimator (Sec. IV B) and a block-dependent maximum likelihood estimator (Sec. IV C). For block-dependent estimators, we also establish confidence intervals for the FD parameter related to inertial range determination. In Sec. V we present an analysis of the aerothermal data that motivated the development of the methodology discussed in previous sections. We summarize the results in Sec. VI.

II. FRACTIONALLY DIFFERENCED PROCESSES

The FD process was originally proposed by Granger and Joyeux [14] and Hosking [15] as an extension to an autoregressive, integrated, moving average model in which the order of integration is allowed to assume noninteger values.

Definition 2.1. Let $\delta \in \mathbb{R}$ and $\sigma_\varepsilon^2 > 0$. We say that $\{X_t\}_{t\in\mathbb{Z}}$ is an FD$(\delta, \sigma_\varepsilon^2)$ if it has a spectral density function (SDF)

$$S_X(f) = \frac{\sigma_\varepsilon^2}{|2\sin(\pi f)|^{2\delta}} \quad |f| < 1/2, \tag{2.1}$$

where σ_ε^2 is the innovation variance, and δ is the fractionally differenced parameter.

When $\delta < 1/2$, an FD process is stationary; when $-1/2 \leqslant \delta < 1/2$, its autocovariance sequence (ACVS) is given by

$$s_{X,\tau} = \frac{\sigma_\varepsilon^2 \sin(\pi\delta)\Gamma(1-2\delta)\Gamma(\tau+\delta)}{\pi\Gamma(\tau+1-\delta)}, \tag{2.2}$$

where $\Gamma(\cdots)$ is Euler's gamma function [16]. When $\delta \geqslant 1/2$, we obtain a class of nonstationary processes that are stationary if $\{X_t\}$ is differenced $d = \lfloor \delta + 1/2 \rfloor$ times, where differencing by d means to form the process $\sum_{k=0}^{d} \binom{d}{k} (-1)^k X_{t-k}$ (e.g., we get $X_t - X_{t-1}$ when $d=1$ and $X_t - 2X_{t-1} + X_{t-2}$ when $d=2$), and $\lfloor x \rfloor$ is the greatest integer less than or equal to x. By inspection of Eq. (2.1), an FD$(\delta, \sigma_\varepsilon^2)$ process approximately obeys a power law process, i.e., $S_X(f) \propto |f|^\alpha$, at low frequencies with $\alpha = -2\delta$ (the error in this approximation is quite small for $|f| \leqslant 1/8$—the range of frequencies that we are interested in for the application discussed below is well below 1/8 in standardized units). For simplicity, we assume that $E\{X_t\} = 0$ throughout (in practice, this assumption does not lose us any generality in what we discuss below because of the differencing operations that are embedded in wavelet filters). It should be noted that an FD process is formulated in discrete time (as opposed to continuous time) so that the highest observable frequency is the Nyquist frequency (1/2 in standardized units). Use of discrete time models avoids nonphysical complications that occur with continuous time power law models that have infinite variance due to an insufficient decay of the SDF as $f \to \infty$ when $\alpha > -1$.

For purposes of studying turbulence data, an FD process has certain advantages over similar models such as fractional Brownian motion (FBM) and fractional Gaussian noise (FGN).

Unlimited power law exponent range. Both FBM and FGN are stochastic power law processes in that their SDF's are approximately proportional to $|f|^\alpha$ at low frequencies; however, an FBM is limited to an exponent range of $-3 < \alpha < -1$ while a FGN is limited to $-1 < \alpha < 1$. An FD process is also a stochastic power law process, but it has no such limitation on its exponent range and is theoretically well defined for $\alpha \in \mathbb{R}$.

Model continuity. Because FBM and FGN jointly cover power laws ranging from -3 up to 1 (adequate to model some—but not all—turbulent phenomena), it is tempting to select between FBM and FGN to model various turbulent series; however, neither model actually includes the case $\alpha = -1$ (known as $1/f$, pink, or flicker noise), and there is a discontinuity between the FGN and FBM models close to $\alpha = -1$ at high frequencies, which can lead to problems in model selection. Unfortunately, many real world phenomena exhibit $1/f$ noise [17]. An FD process has no such discontinuity. In addition, an FD process is closed under differencing operations with regard to its SDF; i.e., an FD$(\delta, \sigma_\varepsilon^2)$ process that has been subjected to a dth order differencing operation, yields an FD$(\delta - d, \sigma_\varepsilon^2)$ process. An FGN or FBM process subjected to the same differencing operation will not yield the same type of process, which is another indication that an FD process is a more flexible and tractable model.

Tractable SDF and ACVS. In contrast to the FBM and FGN models, an FD process has tractable forms for both its SDF and (when stationary) corresponding ACVS; i.e., the

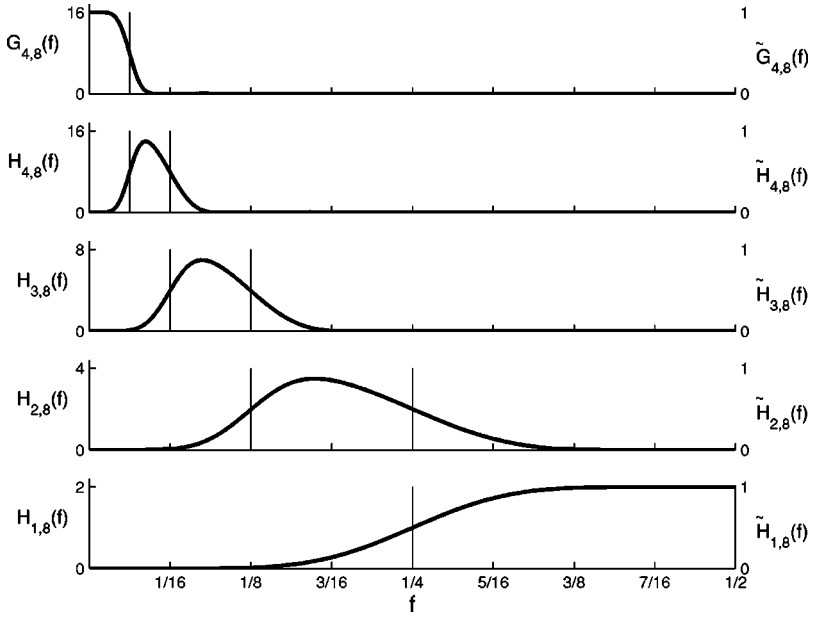

FIG. 1. The squared gain functions for Daubechies least asymmetric eight-tap wavelet filter for levels $j=1,\ldots,4$. For simplicity, the sampling period was set to unity to create the frequency axis and establishes the Nyquist frequency at 1/2. The vertical lines identify the frequency bands with which the wavelet and scaling filters are associated. The scaling of the left (right) ordinate is representative of the DWT (MODWT) squared gain function.

expressions for both the SDF and ACVS of the FD model can be readily computed without having to approximate any infinite summations (this is not true for FGN).

Model flexibility. Both autoregressive and moving average components can be added to an FD process to provide more flexibility in modeling high frequency spectral content, leading to the well-known class of autoregressive, fractionally integrated, moving average models [18]. The high frequency content of measured data is often contaminated by exogenous noise sources, and thus flexible modeling of this region is appropriate. The FBM and FGN models are not readily amenable to such additions as they would further complicate the SDF and ACVS.

III. DISCRETE WAVELET TRANSFORMS

Consider a uniformly sampled time series $\{X_t\}_{t=0}^{N-1}$ with N divisible by 2^J for $J\in\mathbb{N}$. For L an even positive integer, let $\{h_{1,l}\}_{l=0}^{L-1}$ be a Daubechies [19] wavelet filter with squared gain function

$$\mathcal{H}_{1,L}(f)\equiv 2\sin^L(\pi f)\sum_{l=0}^{L/2-1}\binom{L/2-1+l}{l}\cos^{2l}(\pi f). \tag{3.1}$$

Equation (3.1) does not uniquely define a wavelet filter, and an additional phase criterion, such as extremal or least asymmetric phase, must be imposed to do so (use of the latter criterion means that, after an appropriate shift in time, the wavelet filter has approximately zero phase). Let $\{g_{1,l}\}_{l=0}^{L-1}$ be a scaling filter, defined by the quadrature mirror filter relation

$$g_{1,l}=(-1)^{l+1}h_{1,L-1-l}. \tag{3.2}$$

The squared gain function for a Daubechies scaling filter is given by

$$\mathcal{G}_{1,L}(f)\equiv 2\cos^L(\pi f)\sum_{l=0}^{L/2-1}\binom{L/2-1+l}{l}\sin^{2l}(\pi f). \tag{3.3}$$

The wavelet and scaling filters are used in a "pyramid" algorithm [20] to transform $\{X_t\}$ into a collection of wavelet coefficients $W_{j,t}$ and scaling coefficients $V_{j,t}$ that can be associated with scales of, respectively, $\tau_j\equiv 2^{j-1}$ and $2\tau_j$, $j=1,\ldots,J$ (these standardized scales can be converted to physical scales by multiplying them by the sampling time between contiguous observations in $\{X_t\}$). Implementation of the DWT begins by defining the zeroth level scaling coefficients to be the original time series $V_{0,t}\equiv X_t$. The level j wavelet coefficients $W_{j,t}$ and scaling coefficients $V_{j,t}$ are then formed recursively by

$$W_{j,t}\equiv\sum_{l=0}^{L-1}h_{1,l}V_{j-1,2t+1-l \bmod N_{j-1}}, \tag{3.4a}$$

$$V_{j,t}\equiv\sum_{l=0}^{L-1}g_{1,l}V_{j-1,2t+1-l \bmod N_{j-1}}, \tag{3.4b}$$

where $t=0,\ldots,N_j-1$ and $N_j\equiv N/2^j$. For an integer J' satisfying $1\leqslant J'\leqslant J$, we define a level J' DWT of $\{X_t\}$ to be the collection of vectors $\boldsymbol{W}_1,\boldsymbol{W}_2,\ldots,\boldsymbol{W}_{J'},\boldsymbol{V}_{J'}$, where $\boldsymbol{W}_j$ contains the N_j wavelet coefficients $W_{j,t}$, while $\boldsymbol{V}_{J'}$ contains the $N_{J'}$ scaling coefficients $V_{J',t}$.

The pyramid algorithm represented by Eq. (3.4) can also be interpreted as a cascade filter bank operation. Thus an alternative (but less efficient) method for computing $W_{j,t}$ is to subsample what we would get by filtering X_t with a single filter, say $h_{j,l}$, that is the equivalent filter for the cascade filter bank. This filter is an approximate bandpass filter with nominal pass band $f\in[1/4\tau_j,1/2\tau_j]$. The corresponding equivalent scaling filter $g_{j,l}$ used to create the $V_{j,t}$ is a low pass filter with nominal pass band $f\in[0,1/4\tau_j]$. Figure 1

shows the squared gain responses $\mathcal{H}_{j,8}(f)$ for $h_{j,l}$, $j=1,\ldots,4$ and $\mathcal{G}_{4,8}$ for $g_{4,l}$ corresponding to an eight-tap Daubechies wavelet filter $h_{1,l}$ and illustrates the bandpass and lowpass nature of the equivalent wavelet and scaling filters.

When considering the statistical properties of DWT coefficients, it is useful to divide the wavelet and scaling coefficients into boundary and interior coefficients. Boundary coefficients are those subject to change if the ''mod'' operator were to be dropped in Eq. (3.4). These boundary coefficients must be ignored, e.g., when calculating unbiased wavelet variance estimates [see Eq. (4.5) below]. The number of boundary coefficients in $\boldsymbol{W}_j$ or $\boldsymbol{V}_j$ is given by $\min\{L_j',N_j\}$, where $L_j' \equiv \lceil (L-2)(1-2^{-j}) \rceil$, and $\lceil x \rceil$ is the smallest integer that is greater than or equal to x (for large j, $L_j'=L-2$). The remaining $M_j \equiv N_j - \min\{L_j',N_j\}$ coefficients make up the set of interior coefficients. The boundary coefficients are the first N_j-M_j coefficients in $\boldsymbol{W}_j$ or $\boldsymbol{V}_j$, while the interior coefficients are the last M_j elements in these vectors.

A physical interpretation of the DWT based upon Daubechies' class of compactly supported wavelet filters is that the $W_{j,t}$ measure the *difference* (centered at a particular time) between adjacent weighted averages of $\{X_t\}$ at scale τ_j. Large values for the $W_{j,t}$ indicate that $\{X_t\}$ tends to have large variations over time scales of length τ_j. Similar to the wavelet coefficients, the scaling coefficients $V_{j,t}$ are weighted *averages* of $\{X_t\}$ on a scale of $2\tau_j$.

Despite its popularity, the DWT has two practical limitations. The first is the dyadic length requirement. While the DWT can be adapted to accommodate arbitrary length sequences via, e.g., polynomial extensions of the scaling coefficients, selecting an appropriate number of end points to fit or the order of fit is not a trivial task. Other techniques can be used, but generally involve either complicated bookkeeping or are too simple to accurately portray the dynamics of the scaling coefficients. The second limitation is a sensitivity of the DWT to where we start recording a time series; i.e., the decimation operation makes the DWT a non-shift-invariant transform so that circularly shifting the time series can alter the entire DWT.

To overcome these limitations, we can use a nondecimated form of the DWT, known as the maximum overlap DWT (MODWT), that has two main advantages: (1) it handles arbitrary length sequences inherently and (2) circularly shifting the time series will result in an equivalent circular shift of the MODWT coefficients. Additionally, the number of coefficients in each scale is equal to the number of points in the original time series. This refined slicing of the data in combination with the approximate zero phase property of the least asymmetric filters allows us to calculate ''instantaneous'' statistical measures of the data across scales (see Sec. IV B).

As in the DWT, implementation of the MODWT begins by defining the zeroth level scaling coefficients to be the original time series $\tilde{V}_{0,t} \equiv X_t$. Let $\tilde{h}_{1,l} \equiv h_{1,l}/\sqrt{2}$ and $\tilde{g}_{1,l} \equiv g_{1,l}/\sqrt{2}$ for $l=0,\ldots,L-1$. The MODWT wavelet coefficients $\tilde{W}_{j,t}$ and corresponding scaling coefficients $\tilde{V}_{j,t}$ are formed recursively by

$$\tilde{W}_{j,t} \equiv \sum_{l=0}^{L-1} \tilde{h}_{1,l} \tilde{V}_{j-1,t-2^{j-1}l \bmod N}, \tag{3.5a}$$

$$\tilde{V}_{j,t} \equiv \sum_{l=0}^{L-1} \tilde{g}_{1,l} \tilde{V}_{j-1,t-2^{j-1}l \bmod N}, \tag{3.5b}$$

where $t=0,\ldots,N-1$. The collection of vectors $\tilde{\boldsymbol{W}}_1,\tilde{\boldsymbol{W}}_2,\ldots,\tilde{\boldsymbol{W}}_{J'},\tilde{\boldsymbol{V}}_{J'}$ is the level J' MODWT of $\{X_t\}$, where $\tilde{\boldsymbol{W}}_j$ contains the N wavelet coefficients $\tilde{W}_{j,t}$, while $\tilde{\boldsymbol{V}}_{J'}$ has the N scaling coefficients $\tilde{V}_{J',t}$. The number of boundary coefficients in $\tilde{\boldsymbol{W}}_j$ or $\tilde{\boldsymbol{V}}_j$ is $\tilde{L}_j = \min\{(2^j-1)(L-1),N\}$.

If the sample size N is a power of two, the MODWT coefficients and DWT coefficients are related by

$$W_{j,t} = 2^{j/2} \tilde{W}_{j,2^j(t+1)-1} \quad \text{and} \quad V_{j,t} = 2^{j/2} \tilde{V}_{j,2^j(t+1)-1}. \tag{3.6}$$

The DWT can thus be seen as a scaled and subsampled version of the MODWT. As was true for the DWT, we could obtain $\tilde{W}_{j,t}$ by filtering X_t directly with an equivalent MODWT wavelet filter $\tilde{h}_{j,l}$. This filter is related to the corresponding DWT wavelet filter by $\tilde{h}_{j,l} = h_{j,l}/2^{j/2}$, and a similar result holds for the scaling filters. The MODWT squared gain functions are thus given by $\tilde{\mathcal{H}}_{j,L}(f) \equiv 2^{-j}\mathcal{H}_{j,L}(f)$ and $\tilde{\mathcal{G}}_{j,L}(f) \equiv 2^{-j}\mathcal{G}_{j,L}(f)$ (see Fig. 1).

IV. ESTIMATING FD PARAMETERS WITH WAVELETS

Suppose that we have a time series that can be regarded as a realization of a portion $\boldsymbol{X} = [X_0, X_1, \ldots, X_{N-1}]^T$ of an FD$(\delta,\sigma_\varepsilon^2)$ process. In this section we discuss three schemes for estimating the parameter δ via a wavelet transform of $\boldsymbol{X}$. The first two schemes make use of the fact that the relationship between the variance of the wavelet coefficients across scales is dictated by δ in such a manner that we can construct a least squares estimator (LSE) of δ (Abry *et al.* [21,22], Abry and Veitch [23], and Jensen [24] consider similar estimators). The third scheme is a wavelet-based approximation to the maximum likelihood estimator (MLE) of δ (Wornell and Oppenheim [25], Wornell [26,27], Kaplan and Kuo [28], McCoy and Walden [29], and Jensen [30,31] discuss related wavelet-based MLE's). The first LSE and the MLE make use of the entire time series and hence are called ''block-dependent'' estimators; by contrast, the second LSE utilizes only certain coefficients that are colocated in time, and we refer to it as an ''instantaneous'' estimator (this estimator would not change if, e.g., we were to lengthen the time series by prepending it with X_{-1}).

A. Block-dependent weighted least squares estimator

Let $\tilde{\boldsymbol{W}}_j$ be the MODWT wavelet coefficients for scale τ_j. Here we develop a weighted LSE (WLSE) of δ based upon an estimator of the variance of the interior coefficients in $\tilde{\boldsymbol{W}}_j$ over a range of scales τ_j given by $J_0 \leqslant j \leqslant J_1$ (the selection of J_0 and J_1 is application dependent—see Sec. V). Under the

assumption that the length L of the wavelet filter is chosen such that $L/2 \geqslant \lfloor \delta + \frac{1}{2} \rfloor$, these interior coefficients are a portion of a stationary process obtained by filtering $\boldsymbol{X}$ with the equivalent MODWT wavelet filter $\tilde{h}_{j,l}$. Since the squared gain function for $\tilde{h}_{j,l}$ is given by $\tilde{\mathcal{H}}_{j,L}(f)$, the SDF for the interior coefficients is given by $\tilde{\mathcal{H}}_{j,L}(f) S_X(f)$, and hence their variance can be expressed as

$$\nu_X^2(\tau_j) \equiv \mathrm{var}\{\tilde{W}_{j,t}\} = \int_{-1/2}^{1/2} \tilde{\mathcal{H}}_{j,L}(f) S_X(f) df. \tag{4.1}$$

Using the approximation that $\tilde{\mathcal{H}}_{j,L}(f)$ is an ideal bandpass filter over $|f| \in [1/2^{j+1}, 1/2^j]$ and taking into consideration the even symmetry of SDFs, an approximation to the wavelet variance is given by

$$\nu_X^2(\tau_j) \approx 2 \int_{1/2^{j+1}}^{1/2^j} S_X(f) df. \tag{4.2}$$

For fractionally differenced processes, we have

$$\nu_X^2(\tau_j) \approx 2 \int_{1/2^{j+1}}^{1/2^j} \frac{\sigma_\varepsilon^2}{|2 \sin(\pi f)|^{2\delta}} df. \tag{4.3}$$

When $j \geqslant 3$, so that $\sin \pi f \approx \pi f$, Eq. (4.3) can be approximated by

$$\nu_X^2(\tau_j) \approx \sigma_\varepsilon^2 \tilde{c}(\delta) \tau_j^{2\delta - 1}, \tag{4.4}$$

where $\tilde{c}(\delta) \equiv \pi^{-2\delta}(1 - 2^{2\delta - 1})/(1 - 2\delta)$. Equation (4.4) suggests that a direct means of estimating δ is to fit a least squares line to the logarithm of an estimate of the wavelet variance, say $\hat{\nu}_X^2(\tau_j)$. The slope of the line, say β, that best fits $\ln[\hat{\nu}_X^2(\tau_j)]$ versus $\ln(\tau_j)$ in a least squares sense is related to the FD parameter by $\delta = (\beta + 1)/2$ and the power law exponent by $\alpha = -(\beta + 1)$.

Given a time series of length N, we can obtain an unbiased MODWT-based estimate of the wavelet variance by defining

$$\hat{\nu}_X^2(\tau_j) \equiv \frac{1}{\tilde{M}_j} \sum_{t = \tilde{L}_j - 1}^{N-1} \tilde{W}_{j,t}^2, \tag{4.5}$$

where $\tilde{M}_j \equiv N - \tilde{L}_j + 1$ is the number of MODWT interior wavelet coefficients. As a caveat, it should be noted that the wavelet variance estimates are somewhat sensitive to the order L of the wavelet filter used in the analysis. In particular, studies by one of us [32] have shown that there can be a significant bias in estimating δ (and hence α) if we use the Haar wavelet filter (for which $L = 2$). This bias can be attributed to a spectral leakage phenomenon and can be attenuated by increasing L. In practice the choice $L = 8$ works well, so we have used it in all analyses presented in this paper.

The distribution for $\hat{\nu}_X^2(\tau_j)$ is approximately that of a random variable given by $\chi_{\eta_j}^2 \nu_X^2(\tau_j)/\eta_j$, where $\chi_{\eta_j}^2$ is a chi-square random variable with η_j degrees of freedom (Sec. 8.4 of Ref. [32] discusses three methods for determining η_j, the simplest of which is to set $\eta_j = \max\{\tilde{M}_j/2^j, 1\}$). Define

$$Y(\tau_j) \equiv \ln[\hat{\nu}_X^2(\tau_j)] - \psi\left(\frac{\eta_j}{2}\right) + \ln\left(\frac{\eta_j}{2}\right), \tag{4.6}$$

where $\psi(\cdots)$ is the digamma function. The properties of the chi-square distribution dictate that

$$E\{Y(\tau_j)\} = \ln[\nu_X^2(\tau_j)] \quad \text{and} \quad \mathrm{var}\{Y(\tau_j)\} = \psi'(\eta_j/2), \tag{4.7}$$

where $\psi'(\cdots)$ is the trigamma function. By assuming the approximation afforded by Eq. (4.4), we can now formulate a linear regression model $Y(\tau_j) = \gamma + \beta \ln(\tau_j) + e_j$, where $e_j \equiv \ln[\hat{\nu}_X^2(\tau_j)/\nu_X^2(\tau_j)] - \psi(\eta_j/2) + \ln(\eta_j/2)$ defines a sequence of errors, each with zero mean and variance $\psi'(\eta_j/2)$. If we take into account the inhomogeneity in the variance in these errors, we arrive at the WLSE of the slope term β given by

$$\hat{\beta}_{\mathrm{WLSE}} = \frac{\Sigma \omega_j \Sigma \omega_j \ln(\tau_j) Y(\tau_j) - \Sigma \omega_j \ln(\tau_j) \Sigma \omega_j Y(\tau_j)}{\Sigma \omega_j \Sigma \omega_j \ln^2(\tau_j) - [\Sigma \omega_j \ln(\tau_j)]^2}, \tag{4.8}$$

where $\omega_j \equiv [\psi'(\eta_j/2)]^{-1}$, and all sums are over $j = J_0, \ldots, J_1$. The weighted least squares estimate of the FD parameter is then

$$\hat{\delta}_{\mathrm{WLSE}} = \frac{1}{2}(\hat{\beta}_{\mathrm{WLSE}} + 1). \tag{4.9}$$

If we ignore the possible correlation between the error terms (which we can decrease by increasing L), the variance of $\hat{\beta}_{\mathrm{WLSE}}$ is given by

$$\mathrm{var}\{\hat{\beta}_{\mathrm{WLSE}}\} = \frac{\Sigma \omega_j}{\Sigma \omega_j \Sigma \omega_j \ln^2(\tau_j) - [\Sigma \omega_j \ln(\tau_j)]^2}, \tag{4.10}$$

and thus the variance of the $\hat{\delta}_{\mathrm{WLSE}}$ is given by

$$\mathrm{var}\{\hat{\delta}_{\mathrm{WLSE}}\} = \frac{1}{4} \mathrm{var}\{\hat{\beta}_{\mathrm{WLSE}}\}. \tag{4.11}$$

Monte Carlo studies indicate that Eq. (4.10) tends to overestimate the variability in $\hat{\beta}_{\mathrm{WLSE}}$ somewhat and thus can be regarded as a conservative upper bound [32].

B. Instantaneous least squares estimator

The block-dependent WLSE we formulated above depends upon the entire time series $X_0, \ldots, X_{N-1}$. For time series whose statistical properties are evidently evolving over time (such as the aerothermal data considered in Sec. V), the assumptions behind this estimator are violated, and it is problematic to use this estimator on the entire times series. If, however, we can divide the time series up into blocks within which we can assume that the data are the realization of an FD process (with parameters that are now allowed to vary from one block to the next), we can apply the WLSE on

a block by block basis. In practice, each of the blocks will contain the same number of points, so we can now consider N to be the size of each block rather than the length of the entire time series. The choice of N is usually subjective and thus open to question, so it is useful to have some means of verifying that a particular choice is appropriate. We can do so by formulating an ''instantaneous'' estimator that is independent of N and that can be used to check for departures from statistical consistency within a proposed block size.

The idea behind an instantaneous least squares estimate of δ is to use only a single wavelet coefficient from each scale; i.e., we only use $\widetilde{W}^2_{j,t_j}$ to estimate $\nu^2_X(\tau_j)$, where t_j is the time index of the jth level MODWT coefficient associated with time t in $\{X_t\}_{t=0}^{N-1}$. The time index t_j can be meaningfully determined *only* if (approximate) linear phase wavelet filters are used. With this substitution, the time dependent form of Eq. (4.9) becomes

$$\hat{\delta}_{\mathrm{LSE},t}=\frac{\Delta_J\Sigma\ln(\tau_j)Y_t(\tau_j)-\Sigma\ln(\tau_j)\Sigma Y_t(\tau_j)}{2\{\Delta_J\Sigma\ln^2(\tau_j)-[\Sigma\ln(\tau_j)]^2\}}+1/2, \tag{4.12}$$

where $\Delta_J=J_1-J_0+1$, all sums are over $j=J_0,\ldots,J_1$, and

$$Y_t(\tau_j)\equiv\ln(\widetilde{W}^2_{j,t_j})-\psi(1/2)-\ln(2). \tag{4.13}$$

To decrease the variability of the estimates Δ_J should ideally be set to be as large as is feasible.

C. Block-dependent maximum likelihood estimator

Wavelet-based maximum likelihood techniques can be used in harmony with an FD model as another means of obtaining estimates for FD parameters. Using the DWT is advantageous in that it is known to decorrelate long memory FD and related processes, forming a near independent Gaussian sequence, and thus simplifying the statistics significantly [10]. The basic idea is to formulate the likelihood function for the FD parameters δ and σ^2_ε directly in terms of the interior DWT wavelet coefficients. Let $\boldsymbol{W}_I$ be an $M=\Sigma_j M_j$ point vector containing all of the interior DWT wavelet coefficients over a specified range of scales $j=J_0,\ldots,J_1$. We can write the exact likelihood function for δ and σ^2_ε as

$$\mathcal{L}(\delta,\sigma^2_\varepsilon|\boldsymbol{W}_I)\equiv\frac{e^{-\boldsymbol{W}_I^T\Sigma_{\boldsymbol{W}_I}^{-1}\boldsymbol{W}_I/2}}{(2\pi)^{M/2}|\Sigma_{\boldsymbol{W}_I}|^{1/2}}, \tag{4.14}$$

where $\Sigma_{\boldsymbol{W}_I}$ is the covariance matrix of $\boldsymbol{W}_I$, and $|\Sigma_{\boldsymbol{W}_I}|$ is the determinant of $\Sigma_{\boldsymbol{W}_I}$. Note that the dependence of the likelihood function on δ and σ^2_ε is through $\Sigma_{\boldsymbol{W}_I}$ alone. Under the assumption that the wavelet coefficients in $\boldsymbol{W}_I$ are approximately uncorrelated, Eq. (4.14) can be approximated by

$$\widetilde{\mathcal{L}}(\delta,\sigma^2_\varepsilon|\boldsymbol{W}_I)\equiv\prod_{j=J_0}^{J_1}\prod_{t=0}^{M_j-1}\frac{e^{-W^2_{j,t+L'_j}/[2C_j(\delta,\sigma^2_\varepsilon)]}}{[2\pi C_j(\delta,\sigma^2_\varepsilon)]^{1/2}}, \tag{4.15}$$

where $C_j(\delta,\sigma^2_\varepsilon)$ is an approximation to the variance of $W_{j,t}$ given by the average value of the SDF in Eq. (2.1) over the nominal pass band $[1/4\tau_j,1/2\tau_j]$ for the equivalent wavelet filter $h_{j,l}$. The estimate $\hat{\delta}_{\mathrm{MLE}}$ of δ is obtained by maximizing $\widetilde{\mathcal{L}}(\delta,\sigma^2_\varepsilon|\boldsymbol{W}_I)$ with respect to δ. Equivalently we can consider the reduced (natural) log likelihood function

$$\widetilde{l}(\delta|\boldsymbol{W}_I)\equiv M\ln[\widetilde{\sigma}^2_\varepsilon(\delta)]+\sum_{j=J_0}^{J_1}M_j\ln[C'_j(\delta)], \tag{4.16}$$

where $C'_j(\delta)\equiv C_j(\delta,\sigma^2_\varepsilon)/\sigma^2_\varepsilon$ and

$$\widetilde{\sigma}^2_\varepsilon(\delta)\equiv\frac{1}{M}\sum_{j=J_0}^{J_1}\frac{1}{C'_j(\delta)}\sum_{t=0}^{M_j-1}W^2_{j,t+L'_j} \tag{4.17}$$

[see Ref. [32] for explicit details on the development of the reduced (natural) log likelihood function using the DWT coefficients]. Minimizing Eq. (4.16), which is a function of δ alone, yields the maximum likelihood estimate $\hat{\delta}_{\mathrm{MLE}}$, after which we can compute the corresponding estimate for σ^2_ε by plugging $\hat{\delta}_{\mathrm{MLE}}$ into Eq. (4.17).

Under the assumption that $\delta\in[-1/2,L/2]$, the estimator $\hat{\delta}_{\mathrm{MLE}}$ for large M is approximately Gaussian distributed with mean δ and variance

$$\sigma^2_{\hat{\delta}_{\mathrm{MLE}}}\equiv 2\left[\sum_{j=J_0}^{J_1}M_j\phi_j^2-\frac{1}{M}\left(\sum_{j=J_0}^{J_1}M_j\phi_j\right)^2\right]^{-1}, \tag{4.18}$$

where

$$\begin{aligned}\phi_j&\equiv-\frac{4\sigma^2_\varepsilon}{\mathrm{var}\{W_{j,t}\}}\int_0^{1/2}\mathcal{H}_{j,L}(f)\frac{\ln[2\sin(\pi f)]}{[2\sin(\pi f)]^{2\delta}}df\\&\approx-\frac{2^{j+2}}{C'_j(\hat{\delta}_{\mathrm{MLE}})}\int_{1/4\tau_j}^{1/2\tau_j}\frac{\ln[2\sin(\pi f)]}{[2\sin(\pi f)]^{2\hat{\delta}_{\mathrm{MLE}}}}df\end{aligned} \tag{4.19}$$

(see Ref. [11] for details). In practice, the right-hand integral can be approximated through either (i) numerical integration or (ii) a Taylor series expansion about the midband frequencies for levels $j=1,2$ along with direct integration using a small angle assumption for $j>2$. The approximation above is based upon the view that the wavelet transform forms an octave band decomposition. There is generally a large increase in computational speed when using this bandpass approximation with relatively small loss of accuracy.

V. ANALYSIS OF MEASURED AEROTHERMAL TURBULENCE DATA

A. Description of the data

Here we examine a uniformly sampled 7.5 million point aerothermal turbulence data set (referred to as ''aero'' henceforth). These data are a temperature related time series gathered by an aircraft flying at a constant (or linearly increasing) elevation and constant speed in clear air conditions. The measurement system is a cold-wire probe, externally at-

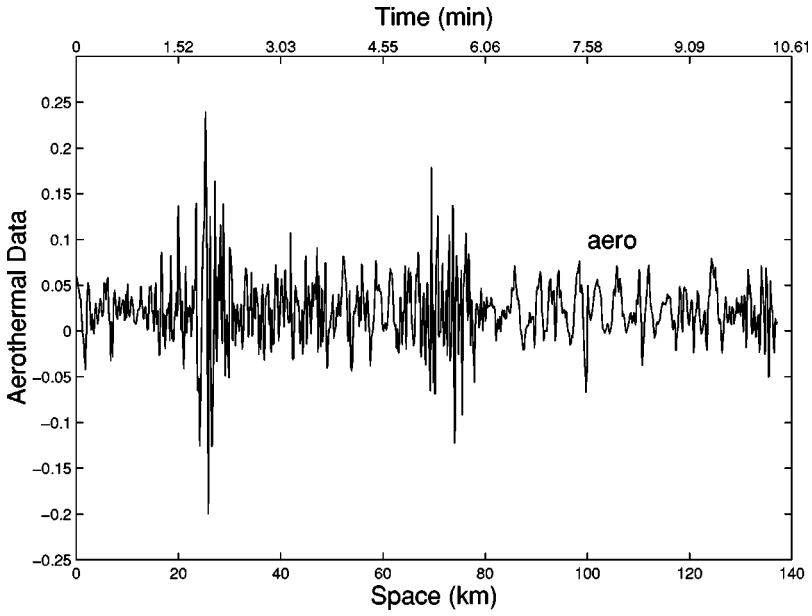

FIG. 2. The aero series smoothed with a MA(10 000,0) filter.

tached to the aircraft, that senses fluctuations in local temperature by means of a proportional change in wire current. The data span a total distance of 137.3 km with a spatial resolution of approximately 1.83 cm. Due to the large amount of data in the aero series, we will use MA(q,r) filters (moving average using windows of length q with an overlap of r points) for purposes of display and comparison of results. Figure 2 shows the aero series smoothed with a MA(10 000,0) filter. Typical of turbulence data, the aero series exhibits seemingly random fluctuations at various scales and times. This particular set of data seems to have a change in some of its characteristics after about 80 km.

B. FD model validation

Figure 3 shows a DWT transform of a small segment of the aero series using Daubechies eight-tap least asymmetric filters, while Fig. 4 shows the corresponding MODWT. The relationship between the DWT and MODWT given in Eq. (3.6) can be visualized, for example, by comparing the DWT scaling coefficients $V_{6,t}$ in Fig. 3 with the corresponding MODWT coefficients $\tilde{V}_{6,t}$ in Fig. 4.

Let us now consider modeling the aero series as the realization of an FD process. We begin by considering some diagnostic statistics designed to help us ascertain if in fact an FD model is appropriate. If this series were an actual realization from an FD process, then, to a good approximation, the interior coefficients in $\boldsymbol{W}_j$ should be a realization of a white noise process [32,10]. To see if this is true, let us look at the sample autocorrelation functions (ACF's) for $\boldsymbol{W}_j$, $j=1,\ldots,11$, of a representative sample of the aero data along with the ACF of the data itself (Fig. 5). Under the white noise hypothesis, standard statistical theory suggests that roughly 95% of the sample ACF values for the wavelet coefficients at scale τ_j should fall between $\pm 2\sqrt{N_j-n}/N_j$, where n is the ACF lag, restricted here to range from 0 to 128 [33]. The actual percentage of coefficients that fall

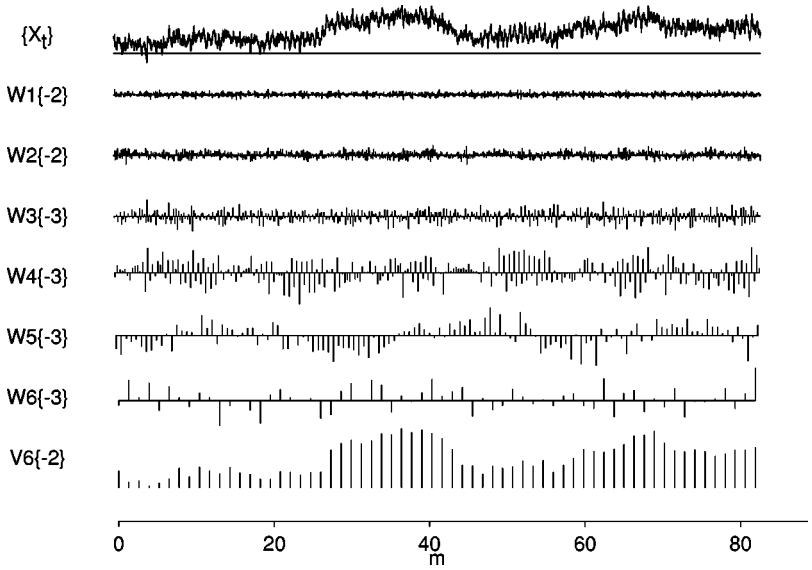

FIG. 3. DWT of aerothermal data segment using Daubechies eight-tap least asymmetric filters. The number in the curly brackets next to each subband represents the amount of circular shift imposed to adjust the coefficients to approximate zero phase. A negative shift value implies an advance, or left circular shift, of the coefficients.

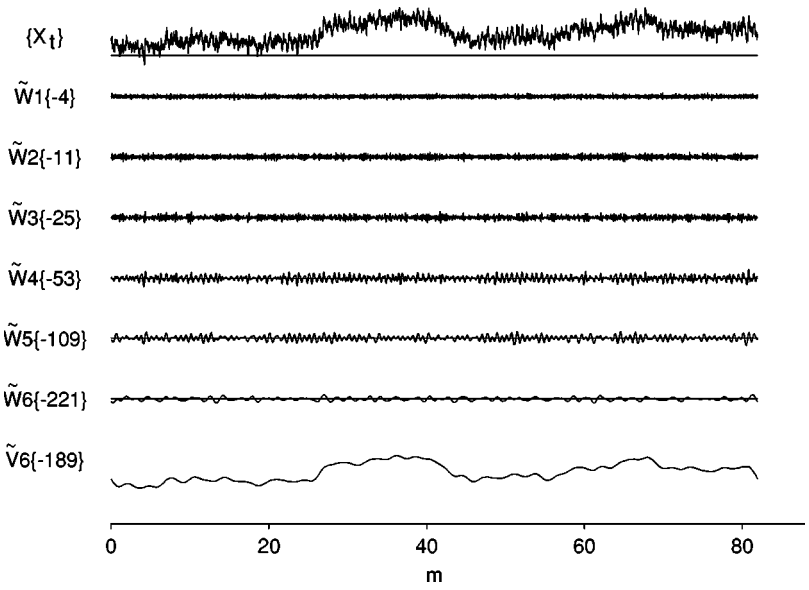

FIG. 4. MODWT of aerothermal data segment using Daubechies eight-tap least asymmetric filters.

within these limits is shown to the right of each plot. The ACF of the aero segment itself shows a persistent positive correlation typical of an FD process; however, the ACF's for $\boldsymbol{W}_1, \ldots, \boldsymbol{W}_5$ exhibit correlation well outside the white noise limits, evidently due to energetic deterministic patterns. This is particularly apparent in the ACF's for $\boldsymbol{W}_4$ and $\boldsymbol{W}_5$, which exhibit a strong (SNR>0.5) sinusoidal beating pattern and pure sine wave pattern, respectively. These periodicities are suspected to be due to an exogenous factor unrelated to aerothermal turbulence such as a periodic autopilot correction or harmonic resonance of the probe armature, inducing a local vibration (and corresponding recorded temperature fluctuation) in the cold wire probe instrumentation. As a result, these deterministic components render an FD model inappropriate over those scales. For scales τ_6 and τ_7, the percentages of sample ACF values falling within the limits are still half to two thirds of the nominal value of 95%, but the values are nonetheless quite small in magnitude (<0.08 for τ_6 and <0.14 for τ_7); for scales τ_8 and above, the percentages are fairly close to 95%. Thus, in keeping with an FD model, the DWT effectively decorrelates the aero segment over scales τ_6 and higher, so this ACF-based diagnostic suggests just applying the FD model over these scales.

Let us now look at a second diagnostic statistic, but based upon the interior MODWT coefficients in $\tilde{\boldsymbol{W}}_j$. Figure 6 shows an example of unbiased wavelet variance estimates for one 2^{16} point block in the aero series. As can be deduced from Eq. (4.4), a multiscale linear pattern in a log-log plot of the wavelet variance versus τ_j would be consistent with the presence of an FD process; however, this figure shows that such linear patterns appear only over a quite limited range of scales. If we segment the log scaled wavelet variance curve into regions over which a linear relationship appears to hold, we obtain a different FD parameter δ over scales $\tau_1 - \tau_4$, $\tau_5 - \tau_7$, and $\tau_8 - \tau_{11}$. These patterns change with different blocks, indicating both time varying and scale dependent power law behavior.

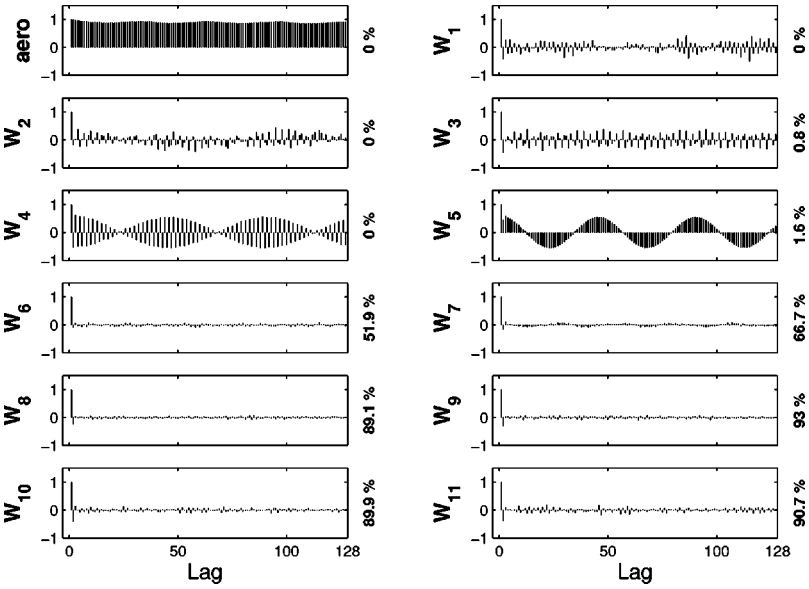

FIG. 5. Biased autocorrelation functions of a 2^{19} point segment of the aero series and of DWT coefficients for $\boldsymbol{W}_1, \ldots, \boldsymbol{W}_{11}$.

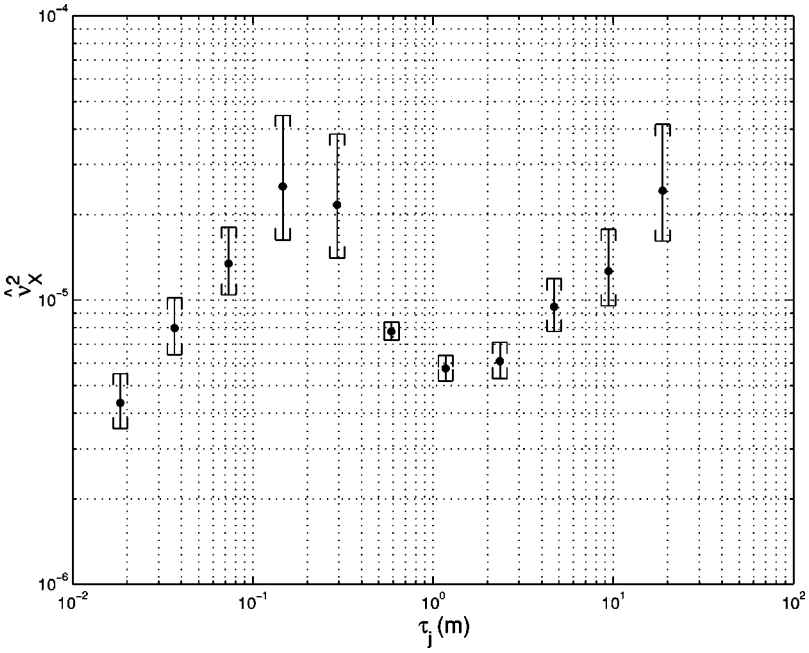

FIG. 6. The unbiased MODWT wavelet variance $\hat{\nu}_X^2(\tau_j)$ of a representative portion of aero using Daubechies least asymmetric eight-tap wavelet filter. The confidence intervals are based on a chi-square distribution assumption where the degrees of freedom are calculated (1) using a large sample approximation to the mean and variance of $\hat{\nu}_X^2(\tau_j)$ for scales $\tau_1, \ldots, \tau_5$ and (2) under an assumption that the SDF is flat over the nominal passbands in which the wavelet coefficients are associated for $\tau_6, \ldots, \tau_{11}$. See Ref. [32] for details of wavelet variance confidence intervals and their development.

Using the collection of diagnostics shown in Figs. 5 and 6, we can demonstrate the methodology described in this paper by fitting separate FD models to the aero series over two finite ranges of scales, namely, $\tau_6 - \tau_8$ and $\tau_9 - \tau_{11}$, each spanning approximately three octaves of frequencies (to simplify our discussion and accompanying figures, we do not consider triads of higher scales).

C. Block-dependent WLSE

Using Eq. (4.9) and the relation $\alpha = -2\,\delta$, the $\hat{\alpha}_{\mathrm{WLSE}}$ were calculated for the aero series over scales $\tau_6 - \tau_8$ and $\tau_9 - \tau_{11}$ (Fig. 7). For simplicity, we define the term $\hat{\alpha}^{\mathrm{WLSE}}_{J_0,J_1}$ to mean the WLSE of the power law exponent over scales $\tau_{J0}, \ldots, \tau_{J1}$. The $\hat{\alpha}^{\mathrm{WLSE}}_{6,8}$ and $\hat{\alpha}^{\mathrm{WLSE}}_{9,11}$ were estimated over contiguous nonoverlapping blocks of size 10 000 and 20 000, respectively. Due to the sampling variability present in the wavelet variance estimates, we smoothed all $\hat{\alpha}^{\mathrm{WLSE}}_{J_0,J_1}$ with a MA(20,19) filter (the choice of this particular filter is somewhat arbitrary, but such smoothing is helpful in making it easier to see how α evolves in time over the two groupings of scales). Note the apparent wide range of $\hat{\alpha}^{\mathrm{WLSE}}_{6,8}$ and $\hat{\alpha}^{\mathrm{WLSE}}_{9,11}$, which roughly span values appropriate for stationary white noise up to nonstationary random walk noise. This clearly suggests that a single (Kolmogorov) exponent is not an adequate description of this aerothermal turbulence data as might be incorrectly construed from conventional Fourier-based methods (see Sec. V F). To quantify this effect we define the inertial range percentage as

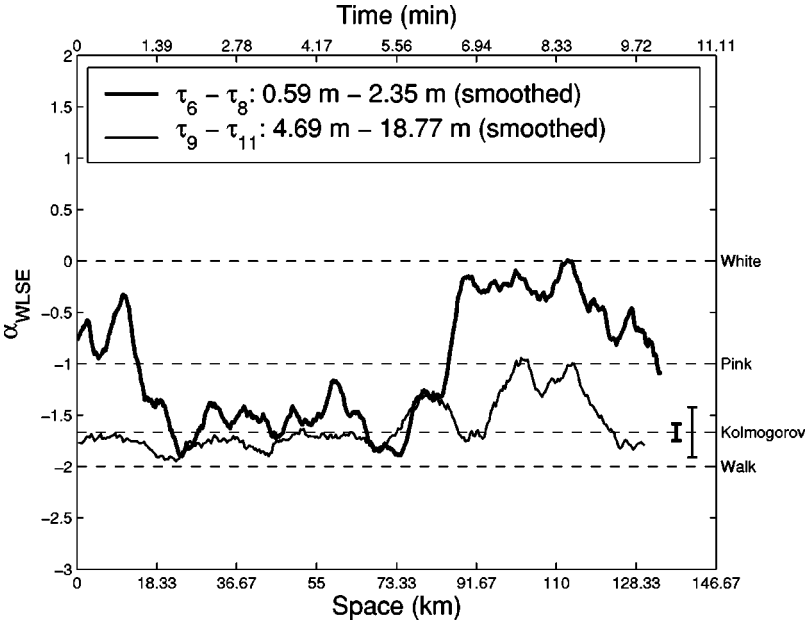

FIG. 7. The $\hat{\alpha}^{\mathrm{WLSE}}_{6,8}$ and $\hat{\alpha}^{\mathrm{WLSE}}_{9,11}$ of the aero series smoothed with a MA(20,19) filter. The confidence limits are for the smoothed estimates shown and are constant since the number of scales over which the estimates are made is constant.

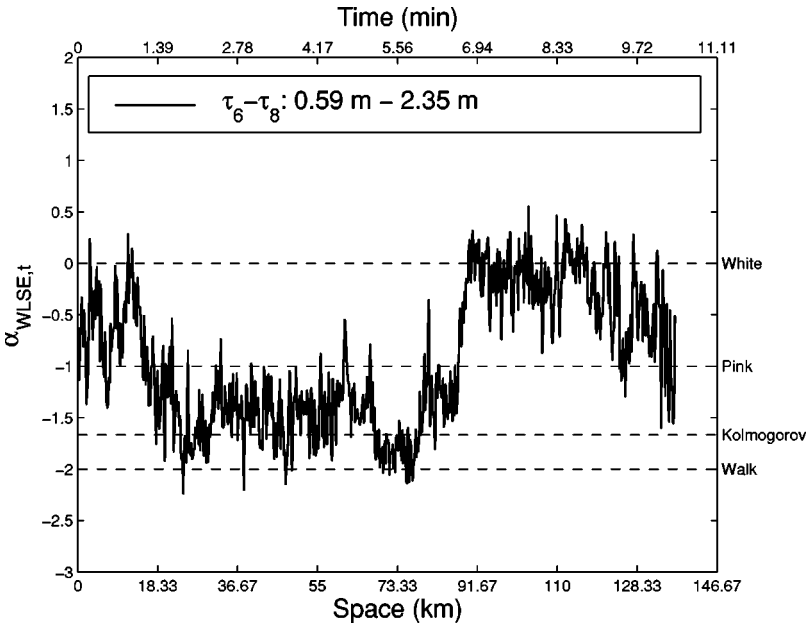

FIG. 8. The $\hat{\alpha}_{\mathrm{LSE},t}$ for the aero series. As a means of comparison with Fig. 7, a MA(10 000,0) filter was used to smooth the results.

$$I_{J_0,J_1} \equiv \frac{100}{P} \sum_{p=1}^{P} U(\mathrm{var}\{\hat{\alpha}_{J_0,J_1,p}\}^{1/2} - |\hat{\alpha}_{J_0,J_1,p} + 5/3|), \tag{5.1}$$

where $U(\cdots)$ is the unit step function and $\hat{\alpha}_{J_0,J_1,p}$ is the $\hat{\alpha}_{J_0,J_1}$ at block p in time. The $I^{\mathrm{WLSE}}_{J_0,J_1}$ represents the percentage of unsmoothed $\hat{\alpha}^{\mathrm{WLSE}}_{J_0,J_1}$ that falls within $\pm\mathrm{var}\{\hat{\alpha}^{\mathrm{WLSE}}_{J_0,J_1}\}^{1/2}$ of the Kolmogorov exponent ($\alpha = -5/3$). Using Eq. (5.1), the inertial range percentages for the WLSE curves were found to be $I^{\mathrm{WLSE}}_{6,8} = 8\%$ and $I^{\mathrm{WLSE}}_{9,11} = 45\%$. Most of the inertial range percentage is achieved where there is a moderate coupling of $\hat{\alpha}^{\mathrm{WLSE}}_{6,8}$ and $\hat{\alpha}^{\mathrm{WLSE}}_{9,11}$ over (approximately) 20–80 km.

D. Block independent (instantaneous) LSE

Instantaneous LSE's of α over scales $\tau_6 - \tau_8$ were calculated for the entire 7.5 million point aero series using Eq. (4.12). Figure 8 shows the $\hat{\alpha}^{\mathrm{WLSE},t}_{6,8}$ smoothed with a MA(10 000,0) filter. These estimates follow the same pattern exhibited by the $\hat{\alpha}^{\mathrm{WLSE}}_{6,8}$ shown in Fig. 7 but with a bit more variability. These variabilities are not captured by the block dependent estimators and illustrate the importance of using time dependent estimators for a more accurate portrayal of the (turbulence) dynamics.

E. Block-dependent MLE

Figure 9 shows the maximum likelihood estimates of α for the aero series smoothed with a MA(20,19) filter. These

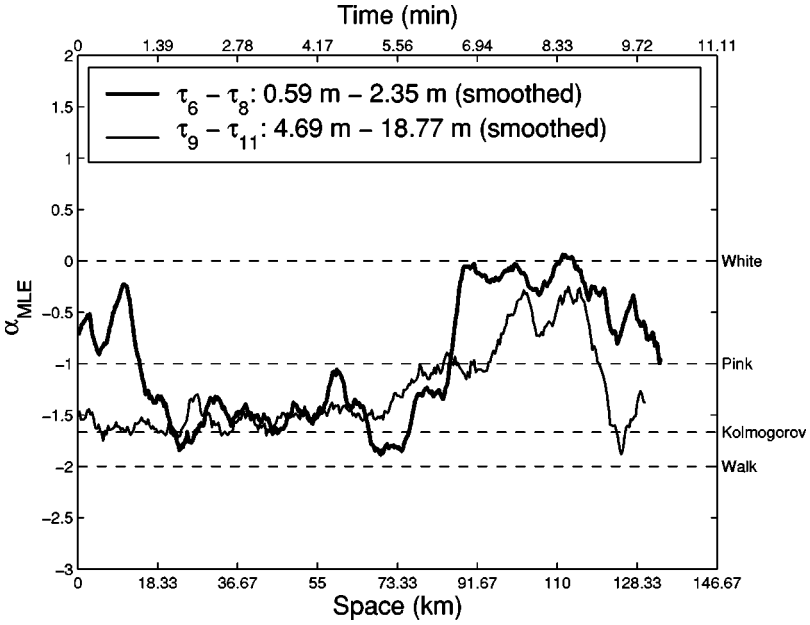

FIG. 9. The $\hat{\alpha}^{\mathrm{MLE}}_{6,8}$ and $\hat{\alpha}^{\mathrm{MLE}}_{9,11}$ of the aero series smoothed with a MA(20,19) filter.

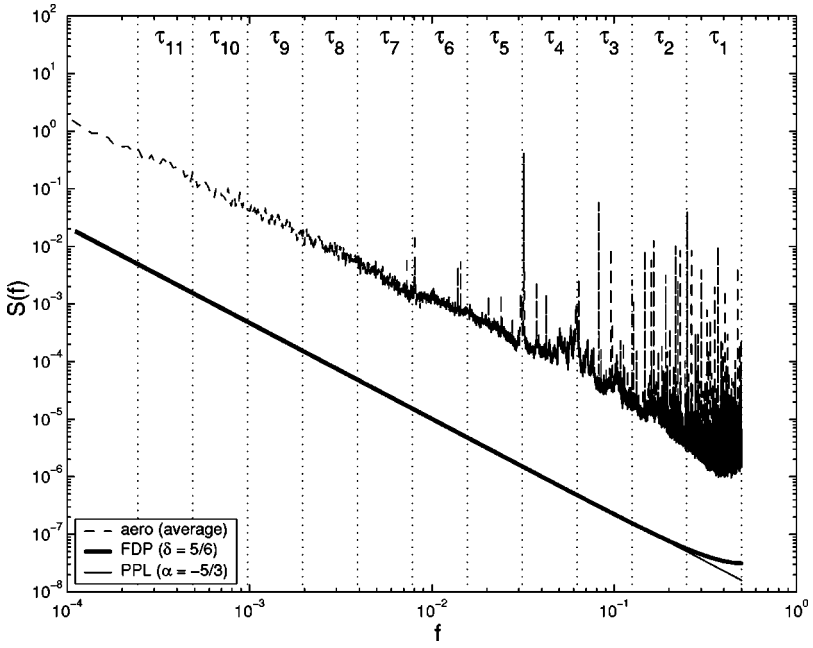

FIG. 10. Averaged estimated SDF for aero series and the theoretical SDF's for an FD process and pure power law (PPL) model of fully developed Kolmogorov turbulence with an infinite inertial range. The FDP and PPL curves are purposefully offset from the average SDF of aero series so that their log-log SDF slopes may be easily compared over a broad range of scale. The vertical divisions represent the octaves over which the wavelet coefficients at scale τ_j are nominally associated.

estimates are noticeably more coupled in the spatial range of 20–80 km than are the $\hat{\alpha}_{\mathrm{WLSE}}$ shown in Fig. 7. Outside of this spatial range, however, both the $\hat{\alpha}_{6,8}^{\mathrm{WLSE}}$ and the $\hat{\alpha}_{6,8}^{\mathrm{MLE}}$ show a strong departure from Kolmogorov turbulence. This change in process dynamics is somewhat discernible in the smoothed plot of the aero series (Fig. 2). The resulting inertial range percentages for the $\hat{\alpha}_{\mathrm{MLE}}$ are $I_{6,8}^{\mathrm{MLE}}=9\%$ $(\approx I_{6,8}^{\mathrm{WLSE}})$ and $I_{9,11}^{\mathrm{MLE}}=22\%$ $(\approx I_{9,11}^{\mathrm{WLSE}}/2)$.

F. Comparison to Fourier techniques

Finally, for contrast, let us look at a common way to analyze turbulence data through an estimate of its SDF. Conventionally, power law exponents are estimated directly from an estimate of the SDF for the data. For example, the slope of the SDF on a log-log scale provides a direct estimate of α. Figure 10 shows the SDF of the entire aero series, computed by partitioning the aero series into 2^{16} point blocks, forming a spectral estimate for each block and then averaging the spectral estimates together. The average SDF portrays a strong Kolmogorov turbulence slope of $\alpha\approx-5/3$ over many octaves. This global approach masks the fact that there are significant deviations from the $-5/3$ law locally in time and hence does not accurately portray the dynamics of α. We could, of course, track the power law estimate of each block as time unfolds, but we would then need some scheme for partitioning the frequencies into regions over which a single power law is applicable. If we use a partitioning scheme that is essentially the same as what our wavelet methodology yields, the work of McCoy *et al.* [29] shows that wavelet-based estimates of α have better mean square error properties than do those based upon the SDF.

VI. DISCUSSION

In this paper we have introduced three wavelet-based techniques to estimate FD model parameters for aerothermal turbulence data: block independent (instantaneous) LSE, and block dependent WLSE and MLE. The block dependent WLSE and MLE verify the presence of time varying power law processes with an estimated power law exponent spanning from white noise to nonstationary red noise and applicable over *finite* ranges of scale. Additionally, averaged block-independent LSE's were shown to match well with block-dependent WLSE's. The LSE's are an effective means of obtaining instantaneous estimates of FD parameters (or, through the approximation $\alpha=-2\delta$, the power law exponents) and are consequently very useful in detecting changes in a system whose dynamics fluctuate rapidly as a function of time or scale. For the block dependent WLSE, we introduced methods for calculating the variance of FD parameter estimates and corresponding confidence intervals. For a specified range of the FD parameter δ and under a large sample assumption, we showed that the block-dependent MLE estimator $\hat{\delta}_{\mathrm{MLE}}$ is approximately Gaussian distributed with mean δ, and we developed the variance of the estimator $(\sigma^2_{\hat{\delta}_{\mathrm{MLE}}})$. To summarize the departure of the estimates from (fully developed) Kolmogorov turbulence, we introduced the inertial range percentage statistic, which quantifies the time and scale dependent intermittency of Kolmogorov turbulence. The collection of results supports the efficacy of using stochastic FD models for aerothermal turbulence data.

ACKNOWLEDGMENTS

This material is based upon work supported by the Air Force Office of Scientific Research under Contract No. F49620-99-C-0068. We would also like to thank Dr. Zhan-Qian Lu of Insightful Corporation for his helpful comments on the manuscript.

[1] F. Moon, *Chaotic and Fractal Dynamics: An Introduction for Applied Scientists and Engineers* (Wiley, New York, 1992).
[2] H. Swinney, Physica D **7**, 3 (1983).
[3] H. Bau and K. Torrance, J. Fluid Mech. **106**, 412 (1981).
[4] N. Aubry, P. Holmes, J. Lumley, and E. Stone, J. Fluid Mech. **192**, 115 (1988).
[5] R. Keolian *et al.*, Phys. Rev. Lett. **47**, 1133 (1981).
[6] M. Vergassola and U. Frisch, Physica D **54**, 58 (1991).
[7] M. Vergassola, R. Benzi, L. Biferale, and D. Pisarenko, J. Phys. A **26**, 6093 (1993).
[8] J. Muzy, E. Bacry, and A. Arneodo, Int. J. Bifurcation Chaos Appl. Sci. Eng. **4**, 245 (1994).
[9] F. Nicolleau and J. Vassilicos, Philos. Trans. R. Soc. London, Ser. A **357**, 2439 (1999).
[10] P. F. Craigmile, D. B. Percival, and P. Guttorp, in *Proceedings of the Third European Conference of Mathematics* (Birkhäuser Verlag, Barcelona, 2000).
[11] P. F. Craigmile, D. B. Percival, and P. Guttorp (unpublished).
[12] G. Katul, M. Parlange, and C. Chu, Phys. Fluids **6**, 2480 (1994).
[13] G. Papanicolaou, K. Solna, and D. Washburn, in *SPIE Conference on Airborne Laser Advanced Technology* (SPIE, Bellingham, WA, 1998), Vol. 3381, pp. 256–267.
[14] C. W. J. Granger and R. Joyeux, J. Time Ser. Anal. **1**, 15 (1980).
[15] J. M. R. Hosking, Biometrika **68**, 165 (1981).
[16] *Handbook of Mathematical Functions*, edited by M. Abramowitz and I. Stegun (U.S. GPO, Washington, DC, 1964).
[17] J. Bassingthwaighte, L. Liebovitch, and B. West, *Fractal Physiology* (Oxford University Press, New York, 1994).
[18] J. Beran, *Statistics for Long-Memory Processes* (Chapman & Hall, New York, 1994).
[19] I. Daubechies, *Ten Lectures on Wavelets*, No. 61 of *CBMS-NSF Series in Applied Mathematics* (SIAM, Philadelphia, 1992).
[20] S. Mallat, IEEE Trans. Pattern Anal. Mach. Intell. **2**, 674 (1989).
[21] P. Abry, P. Gonçalvès, and P. Flandrin, in *Proceedings of the IEEE International Conference on Acoustics, Speech and Signal Processing* (IEEE Press, Minneapolis, 1993), Vol. 3, pp. 237–240.
[22] P. Abry and P. Gonçalvès, in *Wavelets and Statistics*, edited by A. Antoniadis and G. Oppenheim, Lecture Notes in Statistics Vol. 103 (Springer-Verlag, New York, 1995), pp. 15–29.
[23] P. Abry and D. Veitch, IEEE Trans. Inf. Theory **44**, 2 (1998).
[24] M. J. Jensen, J. Forecasting **18**, 17 (1999).
[25] G. W. Wornell and A. V. Oppenheim, IEEE Trans. Signal Process. **40**, 611 (1992).
[26] G. W. Wornell, Proc. IEEE **81**, 1428 (1993).
[27] G. W. Wornell, *Signal Processing with Fractals: A Wavelet-Based Approach* (Prentice Hall, Upper Saddle River, NJ, 1996).
[28] L. M. Kaplan and C.-C. J. Kuo, IEEE Trans. Signal Process. **41**, 3554 (1993).
[29] E. McCoy and A. Walden, J. Comput. Graphical Statistics **5**, 26 (1996).
[30] M. J. Jensen, Stud. Nonlinear Dynamics Econometrics **3**, 239 (1999).
[31] M. J. Jensen, J. Econ. Dynamics Control **24**, 361 (2000).
[32] D. Percival and A. Walden, *Wavelet Methods for Time Series Analysis* (Cambridge University Press, Cambridge, UK, 2000).
[33] W. A. Fuller, *Introduction to Statistical Time Series*, 2nd ed. (John Wiley & Sons, New York, 1996).